



1 **Technical Note: Monte-Carlo genetic algorithm (MCGA) for**
2 **model analysis of multiphase chemical kinetics to determine**
3 **transport and reaction rate coefficients using multiple**
4 **experimental data sets**

5

6 **Thomas Berkemeier^{1,*}, Markus Ammann², Ulrich K. Krieger³, Thomas Peter³, Peter**
7 **Spichtinger⁴, Ulrich Pöschl¹, Manabu Shiraiwa^{1,5} and Andrew J. Huisman⁶**

8 [1] Max Planck Institute for Chemistry, Multiphase Chemistry Department, 55128, Mainz,
9 Germany

10 [2] Paul Scherrer Institute, Laboratory of Environmental Chemistry, 5232, Villigen, Switzerland

11 [3] ETH Zurich, Institute for Atmospheric and Climate Science, 8092, Zurich, Switzerland

12 [4] Johannes Gutenberg University, Institute for Atmospheric Physics, 55128, Mainz, Germany

13 [5] University of California Irvine, Department of Chemistry, 92697, Irvine, CA, USA

14 [6] Union College, Department of Chemistry, 12308, Schenectady, NY USA

15 *now at: Georgia Institute of Technology, School of Chemical and Biomolecular Engineering,
16 30320, Atlanta, GA, USA

17

18 **Corresponding Authors:** T. Berkemeier (thomas.berkemeier@chbe.gatech.edu) and A. J.

19 Huisman (huismana@union.edu)



20 **Abstract**

21 We present a Monte-Carlo Genetic Algorithm (MCGA) for efficient, automated and unbiased
22 global optimization of model input parameters by simultaneous fitting to multiple experimental
23 data sets. The algorithm was developed to address the inverse modelling problems associated with
24 fitting large sets of model input parameters encountered in state-of-the-art kinetic models for
25 heterogeneous and multiphase atmospheric chemistry. The MCGA approach utilizes a sequence
26 of optimization methods to find the solution of an optimization problem and to explore the space
27 of solutions with similar model output. It addresses a problem inherent to complex models whose
28 extensive input parameter sets might not be uniquely determined from limited input data. Such
29 ambiguity in the derived parameter values can be reliably detected using this new set of tools. The
30 MCGA algorithm has been used successfully to constrain parameters such as reaction rate
31 coefficients, diffusion coefficients and Henry's law solubility coefficients in kinetic models of gas
32 uptake and chemical transformation of aerosol particles as well as multiphase chemistry at the
33 atmosphere-biosphere interface. It should be portable to any numerical model with similar
34 computational expense and extent of the fitting parameter space.

35

36 **1. Introduction**

37 Atmospheric aerosols play a key role in climate, air quality and public health. Heterogeneous
38 reactions and multiphase processes alter the physical and chemical properties of organic aerosol
39 particles, but the effects of these reactions are not fully elucidated (e.g. Finlayson-Pitts,
40 2009;George and Abbatt, 2010;Abbatt et al., 2012;Pöschl and Shiraiwa, 2015). While multiphase
41 chemistry in aerosols and clouds can be described by a sequence of well-understood physical and



42 chemical elementary processes in kinetic models (Hanson et al., 1994;Pöschl et al., 2007;George
43 and Abbatt, 2010), the deduction of parameters or rate coefficients of the individual elementary
44 processes is severely complicated by the inherent coupling of chemical reactions and mass
45 transport processes (Kolb et al., 2010;Berkemeier et al., 2013;Shiraiwa et al., 2014).

46 Heterogeneous chemical reactions on aerosol particles are traditionally described using so-called
47 "resistor" models, which represent parallel and sequential physical or chemical processes in
48 analogy to electrical circuits. These models have typically been used to derive analytical
49 expressions for simplified limiting cases (e.g. Hanson et al., 1994;Worsnop et al., 2002;Hearn et
50 al., 2005). Recently, numerical models have been developed that allow a more complete
51 consideration of the time- and depth-resolved chemical and physical behaviour of aerosol particles,
52 leading to a better understanding of these reaction systems, especially under conditions where the
53 steady-state assumptions underlying the resistor models are not valid (Smith et al., 2003;Pöschl et
54 al., 2007;Steimer et al., 2015;Berkemeier et al., 2016). Kinetic multi-layer models describe single
55 particles or thin films by division into compartments such as near-surface gas phase, surface and
56 particle bulk, and further subdivision of the particle bulk into thin layers to achieve depth-
57 resolution. Specific models provide a focus on chemistry such as KM-SUB (Shiraiwa et al., 2010),
58 on gas-particle partitioning such as KM-GAP (Shiraiwa et al., 2012) and ADCHAM (Roldin et al.,
59 2014), or on water diffusion such as the ETH Diffusion Model (Zobrist et al., 2011). For simplicity,
60 throughout this manuscript we refer to a "kinetic model" as any computational model that is used
61 to simulate a system's behaviour and to "input parameters" as any parameters (thermodynamic,
62 kinetic, or physical) that need to be optimized so that the kinetic model accurately represents
63 experimental data.



64 Ideally, fitting a kinetic model to experimental data would return all chemical and physical
65 parameters necessary to understand the importance of the processes at work and to predict the
66 outcome of future experiments, even if conducted under experimental conditions not part of the
67 training data set, i.e. all experimental data used during the fitting process. However, kinetic models
68 often require a multitude of input parameters, some of which are not constrained well
69 experimentally or are merely effective parameters combining a sequence of inherently coupled
70 processes. In general, two main difficulties arise when optimizing complex models to experimental
71 data:

72 (1) The optimization hyper surface is often non-convex, i.e., it will not have only a single minimum
73 due to interactions between non-orthogonal input parameters and/or scatter in the experimental
74 data. Hence, steepest descent methods fail since they get trapped easily in local minima. Brute-
75 force or exhaustive searches, where an n -dimensional grid is applied to the input parameter space
76 and the fit quality evaluated for every grid point in all n dimensions, are often not computationally
77 feasible.

78 (2) If too little or too similar experimental data is used during the fitting process or input
79 parameters are allowed to move in a large range, the optimization problem can be underdetermined
80 (ill-defined) and multiple solutions may exist. In this case, even though a good agreement between
81 model output and training data set is obtained, it is likely that only the model input parameters
82 corresponding to the most limiting processes will be physically meaningful. Extrapolation of the
83 model outside its training range can then lead to strong discrepancies between modelled and
84 measured data.



85 Hence, sophisticated optimization methods are needed, which quickly and reliably determine the
86 model input parameters that lead to the best correlation between model and experimental data.
87 Furthermore, experiments must be conducted by covering broad ranges of experimental conditions
88 to achieve that the observables are controlled by (a) as many model input parameters as possible
89 across all experimental conditions, but (b) by as few model input parameters as possible for a
90 specific experimental condition (i.e. limiting cases). Note here that technical limitations or
91 transient behaviour of a reaction system may not allow probing the entirety of the parameter space
92 in the required breath.

93

94 **2. Monte-Carlo Genetic Algorithm (MCGA)**

95 In many modelling applications, methods are needed that reliably find the optimum in non-convex
96 optimization problems and detect underdetermined optimization problems. Global optimization
97 methods have been subject of extensive research in the past (Arora et al., 1995) and provide means
98 of approximating non-convex optimization problems without premature convergence to local
99 optima. Examples for these methods are simulated annealing methods and evolutionary
100 algorithms. In atmospheric chemistry, simple optimization techniques are commonly used to
101 determine kinetic parameters by fitting of rate equations to experimental data sets, but to our
102 knowledge no global optimization technique diligently designed for the determination of
103 atmospheric reaction rate coefficients from multiple data sets was described thus far. For cloud-
104 aerosol interaction models, inverse modeling techniques using evolutionary algorithms as global
105 optimization technique in Monte-Carlo Markov Chain (MCMC) algorithms were developed
106 previously to determine parametric uncertainties (Partridge et al., 2012;Lowe et al., 2016). Global



107 optimization was also used to calculate thermodynamic equilibria for phase separation of aqueous
108 multicomponent solutions (Zuend and Seinfeld, 2013).

109 In this study, we present the Monte-Carlo Genetic Algorithm (MCGA), a method combining direct
110 Monte-Carlo sampling with a genetic algorithm as heuristic global optimization method that
111 approximates the global optimum for input parameter sets of computational models. Repeated
112 execution of the search algorithm can be used to test for uniqueness or to provide statistical bounds
113 on the model input parameters. The MCGA algorithm utilizes a two-step approach to find minima
114 on non-convex hyper surfaces. First, a Monte-Carlo (MC) sampling is performed in the large space
115 of possible model input parameters to narrow down the possible solution to smaller areas of
116 interest. The parameter sets are evaluated using a goodness-of-fit expression of the user's choice,
117 such as the root-mean-square (RMS) error. In the examples presented here, the RMS error or
118 logarithmic RMS error was used. When multiple datasets were fitted, a weighting factor was
119 introduced to prevent bias due to the number of data points in different experimental datasets. An
120 additional optional weighting factor allows the user to assign priority to experimental data with
121 lower statistical error or scatter. The parameter sets for the MC sampling are generated randomly
122 from a distribution of the model input parameters. Each parameter was sampled using a
123 logarithmically spaced distribution of values to provide uniform sampling over the large ranges
124 most input parameters can possibly adopt. Note that, depending on the problem, different
125 distributions and sampling strategies (e.g. Latin hypercube sampling) could be applied.

126 The genetic algorithm (GA) uses survival of the fittest to optimize an ensemble (the *population*)
127 of parameter sets (the *individuals*) over several iterations (the *generations*). Processes known from
128 natural evolution such as survival, recombination, mutation and migration are mimicked to
129 optimize a population. The initial population is formed by the parameter sets with the best



130 goodness-of-fit obtained in the MC sampling step. An equal number of random parameter sets are
131 added to ensure diversity within the pool of parameter sets and counteract sampling bias from
132 shallow local minima (Fig. 1).

133 During execution of the GA, a number of model input parameter sets with the highest correlation
134 between model output and experimental data (goodness-of-fit) are directly transferred into the next
135 generation by the survival mechanism (the *parents*). The remaining population is recombined to
136 generate new combinations of parameters from the existing sets, forming the *children* for the next
137 generation. To further ensure genetic variability, a mutation scheme alters parameters in a
138 stochastic manner. For the same purpose, the MCGA code allows for optional reseeding of a
139 population during optimization, i.e. replacing random individuals in the population with random
140 or pre-sampled individuals from the preceding MC run, and for optional migration between
141 different populations if multiple subpopulations are being evolved concurrently. Collectively,
142 these mechanisms enable the MCGA to overcome local minima, a crucial feature of a global
143 optimization method. Iteration of these steps eventually results in a homogeneous, optimized
144 population and the common parameter set is taken as result. In lieu of reseeding and migration,
145 MCGA can be run multiple times to generate a set of representative solutions, which has been the
146 default approach in previous applications of MCGA (cf. Sect. 4). With only few (~5-10)
147 repetitions, this procedure allows the user to assure full convergence to the global optimum. In
148 addition, the random sampling of optimization space between different executions of MCGA will
149 generate statistical bounds on the parameters if a sufficiently large number of repetitions is
150 computationally feasible.



151 In this study we used the genetic algorithm provided by MathWorks® (Matlab® Global
152 Optimization Toolbox) and developed a routine for parallel computation on computer clusters. In
153 a typical setting, the MC step and GA step of the optimization occupied an approximately equal
154 amount of computation time. Figure 2 describes the implementation of the parallel MCGA
155 optimization method. The N parallel threads share common populations of parameter sets that are
156 iteratively optimized by extracting a subset of parameter sets and performing the genetic algorithm
157 on this subset. Once a sub-evaluation of the genetic algorithm has finished, the parameter sets are
158 mixed into the population, and after randomization, a different subset of parameter sets is extracted
159 and their optimization is immediately continued. Since the parallel threads will run
160 asynchronously, a fraction of individuals must remain in the population to be mixed with, to enable
161 continuous operation without waiting times.

162

163 **3. Implications for modelling and measuring chemical kinetics**

164 Although models may possess a multitude of kinetic and thermodynamic input parameters that
165 represent the many possible sequential and/or concurrent processes occurring in the system, their
166 behaviour is often driven by only a single or at most a few processes at a certain point in time. In
167 chemical kinetics, the behaviour of the system can often be characterized by a kinetic regime,
168 which may change during the course of the reaction and with experimental conditions (Berkemeier
169 et al., 2013). If a set of model input parameters can be uniquely determined (by MCGA or another
170 means) and results in a high-fidelity fit of model output to experimental data, the parameters then
171 would be regarded as correct within the approximations of the underlying model and uncertainties
172 of the experimental data. This is a convenient way to assimilate data from multiple previous



173 studies; data sets can be weighted to reflect confidence in their results, and the final range of
174 accepted parameters then represents a consensus from the fitted data. However, it may not always
175 be possible to fully constrain the input parameters, even using multiple experimental datasets. In
176 general, there are two reasons that a model input parameter can remain unconstrained after
177 optimization:

- 178 (i) the parameter is non-influential, or
- 179 (ii) the parameter is inherently coupled to another one, forming a non-orthogonal parameter
180 pair under all experimental conditions.

181 Fig. 3 illustrates both cases in an example taken from atmospheric multiphase chemistry, using the
182 benchmark system of ozone + oleic acid and data adopted from Hearn *et al.* (2005). The original
183 data was converted from ozone exposure to a time series using an ozone concentration of 2.76×10^{15}
184 cm^{-3} . The MCGA algorithm was executed under a constrained parameter set, in which only
185 desorption lifetime and surface reaction rate coefficient were allowed to vary. In this scenario,
186 repeated execution of MCGA returned multiple solutions, for which the model output had nearly
187 equivalent goodness-of-fit with only slight variance between them (Fig. 3A). In stark contrast to
188 the uniform correlation between model output and experimental data, Fig. 3B shows the high
189 variance within the model parameters yielding these solutions (red markers) which scatter across
190 a narrow valley of the optimization hypersurface (contour lines). In the upper portion of the figure,
191 i.e. above a desorption lifetime of 10^{-4} s, a vertical relationship between both parameters indicates
192 that the desorption lifetime is a non-influential parameter and can take on any value in this interval,
193 corresponding to case (i) above. In the lower portion of the figure, i.e. below a desorption lifetime
194 of the diagonal relationship indicates that an increase in one parameter can be compensated with a
195 decrease in the other parameter and both form a non-orthogonal pair, corresponding to case (ii)



196 above. For comparison, Figs. 3C and 3D show examples of optimization hypersurfaces from
197 Berkemeier et al. (2016), who studied multiphase ozonolysis of shikimic acid and investigated the
198 existence of non-orthogonal parameter pairs by varying optimized parameters (λ_i) by a factor $f(\lambda_i)$
199 to depict the total residual as a 2D contour map. Fig. 3C shows that the Henry's law coefficient for
200 ozone (H_{ep,O_3}) and the product of the bulk reaction rate coefficient (k_{BR}) with the bulk diffusivity
201 of ozone (D_{b,O_3}) and the bulk-to-surface transport coefficient of ozone (k_{bs,O_3}) are fully non-
202 orthogonal. Figure 3D shows a single, well-defined optimum parameter set for the effective
203 molecular cross section of ozone (σ_{O_3}) and the desorption lifetime of ozone (τ_{d,O_3}), indicating that
204 these parameters are fully orthogonal for the experimental data fit in that study.

205 The prerequisite of a successful optimization is to fit a sufficiently broad experimental data set so
206 that a unique and accurate set of fitting parameters is obtained. Thus, both of the above conditions
207 must be avoided. This may be achieved by including additional experimental data, especially from
208 a different experimental technique or over a different timescale so that the system might sample
209 another limiting behaviour. In the data given in Fig. 3 above, for example, measuring full time
210 series at different oxidant concentrations may help to constrain the oxidant's desorption lifetime.
211 However, if a model has too many free parameters (or especially parameters that are not well-
212 constrained by experimental data), it may be necessary to reduce the model complexity or fix some
213 of the parameters. We therefore recommend using data sets obtained from a range of different
214 experimental techniques to ensure this variability if they are available, and using models with as
215 few free parameters as possible.

216 In the example above, it was possible to use brute-force sampling to determine the true
217 optimization hypersurface (contour lines) for comparison to the MCGA results. Of course, in
218 typical applications, the number and range of input parameters makes such a search prohibitive.



219 The computational feasibility of an optimization depends crucially on the size of the input
220 parameter space, i.e. number and possible range of all parameters. Using an unreasonably large
221 range for input parameters increases the possibility of finding non-physical solutions that fit the
222 experimental data. The input parameter space can be reduced based on *a priori* knowledge from
223 laboratory experiments and theoretical calculations. Parameters can be narrowed down by
224 laboratory experiments (e.g. bulk experiments for derivation of trace gas solubility), by physics
225 (e.g. the upper limit of the accommodation coefficient at unity), or by simulations (e.g., molecular
226 dynamics simulations to estimate the surface accommodation coefficient and desorption lifetime
227 as in Vieceli et al. (2005) and Julin et al. (2013)). Note that in the example given in Fig. 3b, the
228 two parameters were not truly independent, so that constraining either model parameter from *a*
229 *priori* information would constrain the other parameter. In multi-parameter optimizations, where
230 many such dependencies might exist, this can lead to a significant reduction in solution space.

231

232 4. Application of MCGA in atmospheric multiphase chemistry

233 The MCGA algorithm has been applied previously to chemical reaction systems of atmospheric
234 relevance (Table 1). The essential parameters we use to describe an atmospheric multiphase
235 chemical kinetic system of reactive trace gases X and bulk material Y include chemical reaction
236 rate coefficients at the surface (k_{SLR}) and in the bulk (k_{BR}) of aerosol particles; bulk diffusion
237 coefficients of reactive trace gases (D_X) and the bulk matrix (D_Y); accommodation coefficients
238 ($\alpha_{s,X}$) and desorption lifetimes ($\tau_{d,X}$) of trace gases to the particle surface to determine transient and
239 equilibrium adsorption behavior; and equilibrium constants for the solubility of reactive trace



240 gases ($K_{\text{sol,cc},X}$), typically expressed in terms of Henry's law coefficients ($H_{\text{cp},X}$) (Pöschl et al.,
241 2007; Ammann and Pöschl, 2007; Shiraiwa et al., 2010; Berkemeier et al., 2013).

242 In its first application the MCGA algorithm was used to fit individual data sets of the decay of
243 oleic acid upon ozonolysis (Berkemeier et al., 2013), highlighting the need of fitting to multiple
244 experimental data sets to constrain kinetic parameters. This was done in further studies that
245 investigated gas uptake to (semi-)solid organic material in coated-wall flow-tube reactors (Arangio
246 et al., 2015; Berkemeier et al., 2016), ozone-induced protein oligomerization in bulk solutions
247 (Kampf et al., 2015), viscosity change upon alkene ozonolysis as measured with fluorescence
248 microscopy (Hosny et al., 2016) as well as the redox-cycling reactions in the human lung lining
249 fluid (Lakey et al., 2016). In each of these studies, a large set of model input parameters was
250 optimized to several kinetic data sets to constrain the input parameter space. In the following, we
251 review results previously obtained by the MCGA algorithm to demonstrate its utility in
252 determining kinetic parameters, assimilating large datasets, and detecting ill-defined problems.

253 In Berkemeier et al. (2016), 11 parameters were varied simultaneously to fit the ozone uptake to
254 shikimic acid films over many hours, under 12 distinct experimental conditions, and using a single
255 set of kinetic parameters (Fig. 4). The model was found to accurately describe the humidity- and
256 concentration-dependence of ozone uptake and a high correlation between model output and
257 experimental data was achieved. During optimization, a subset of six parameters, including
258 diffusivity coefficients and trace gas solubility, was allowed to increase or decrease monotonically
259 over 6 steps in relative humidity, resulting in a total of 41 optimized parameter values. Despite this
260 large number of optimization parameters, a well-constrained parameter set could be obtained due
261 to the large depth in training data and by applying *a priori* information.



262 In another study investigating the oxidation of biomass burning tracers with hydroxyl radicals
263 (Arangio et al., 2015), repeated execution of MCGA revealed a remaining uncertainty in the kinetic
264 parameters obtained from optimization to the two experimental data sets (Fig. 5). While some
265 parameters could be narrowly constrained (diffusion coefficient of the organic matrix, D_{org}), others
266 were subject to larger uncertainties (surface layer reaction rate constant k_{SLR} , desorption lifetime
267 τ_d). Note that while these parameters seem almost unconstrained in Fig. 5, this uncertainty is due
268 to the presence of non-orthogonal parameter pairs. As detailed in Fig. 3 and in Arangio et al.
269 (2015), only specific combinations of the non-orthogonal parameters will lead to agreement
270 between model and experiment. This knowledge can be used to constrain these parameters in
271 further experiments.

272 5. Conclusions

273 The MCGA algorithm addresses the problem of extracting physical and chemical parameters from
274 experimental data. The algorithm allows the user to assimilate multiple datasets and its random
275 sampling approach reduces the bias which may arise in more user-directed optimization methods.
276 Unlike simple gradient-based optimization methods, MCGA can thus be used as a statistical tool
277 that not only detects unconstrained parameters, but also finds dependencies between unconstrained
278 parameters. The results can be applied in process models and may serve to direct future
279 experimental studies, e.g. to drive a reaction system into regimes in which the remaining
280 unconstrained parameters have high sensitivity. MCGA could also be used to constrain chemical
281 reaction systems in the post-analysis of field and laboratory studies: starting with a large set of
282 model input parameters (i.e. chemical reactions, physical processes), data from various
283 measurement campaigns could be combined, reconciled and in a further step used to reduce the
284 number of model input parameters to the key processes necessary to describe all measurement



285 data. MCGA may be a powerful and useful tool to constrain kinetic parameters and reaction rate
286 coefficients in models that study the formation of secondary organic aerosol in reaction chambers
287 (Chan et al., 2007; Shiraiwa et al., 2013; Cappa et al., 2013; Riedel et al., 2016). It could be suitable
288 for fine-tuning of reaction rates in large reaction mechanisms of atmospheric chemistry, such as
289 the Master Chemical Mechanism (MCM; Jenkin et al., 1997; Saunders et al., 2003), the Gas-
290 Aerosol Model for Mechanism Analysis (GAMMA; McNeill et al., 2012) or the Chemical
291 Aqueous Phase Radical Mechanism (CAPRAM; Herrmann et al., 1999). Multiple experimental
292 data sets from a broad range of techniques could be used with the algorithm to narrow down
293 difficult-to-measure reaction rate coefficients, provide uncertainty estimates and reconcile
294 experiments across different research groups and facilities.

295 **Acknowledgements**

296 T. Berkemeier was supported by the Max Planck Graduate Center with the Johannes Gutenberg-
297 Universität Mainz (MPGC). A. J. Huisman was supported by the United States National Science
298 Foundation under award no. IRFP 1006117 and by ETH Zürich. Any opinions, findings, and
299 conclusions or recommendations expressed in this material are those of the authors and do not
300 necessarily reflect the views of the US National Science Foundation. We gratefully acknowledge
301 G. D. Smith for providing published data in tabulated form. The authors like to thank A. Pozzer,
302 C. Pfrang and C. Marcolli for stimulating discussions and support.



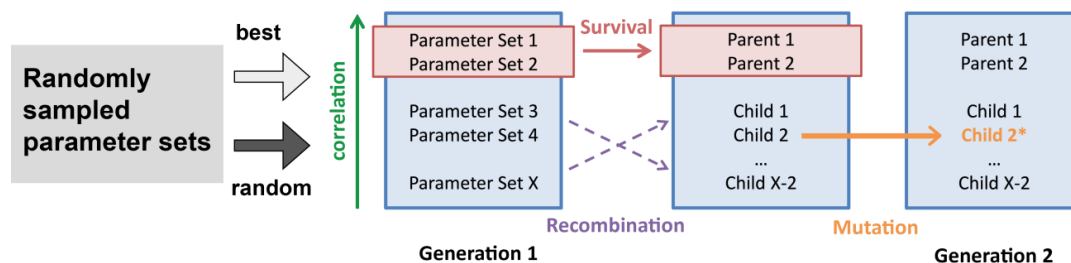
303 **Table 1.** Previous studies applying the MCGA algorithm.

Study	Reaction system
Berkemeier et al. (2013)	oleic acid + O ₃
Arangio et al. (2015)	levoglucosan and abietic acid + OH
Kampf et al. (2015)	protein + O ₃
Hosny et al. (2016)	oleic acid + O ₃
Berkemeier et al. (2016)	shikimic acid + O ₃
Tong et al. (2016)	OH formation by SOA decomposition in water
Lakey et al. (2016)	reactive oxygen species and PM _{2.5} in lung lining fluid

304

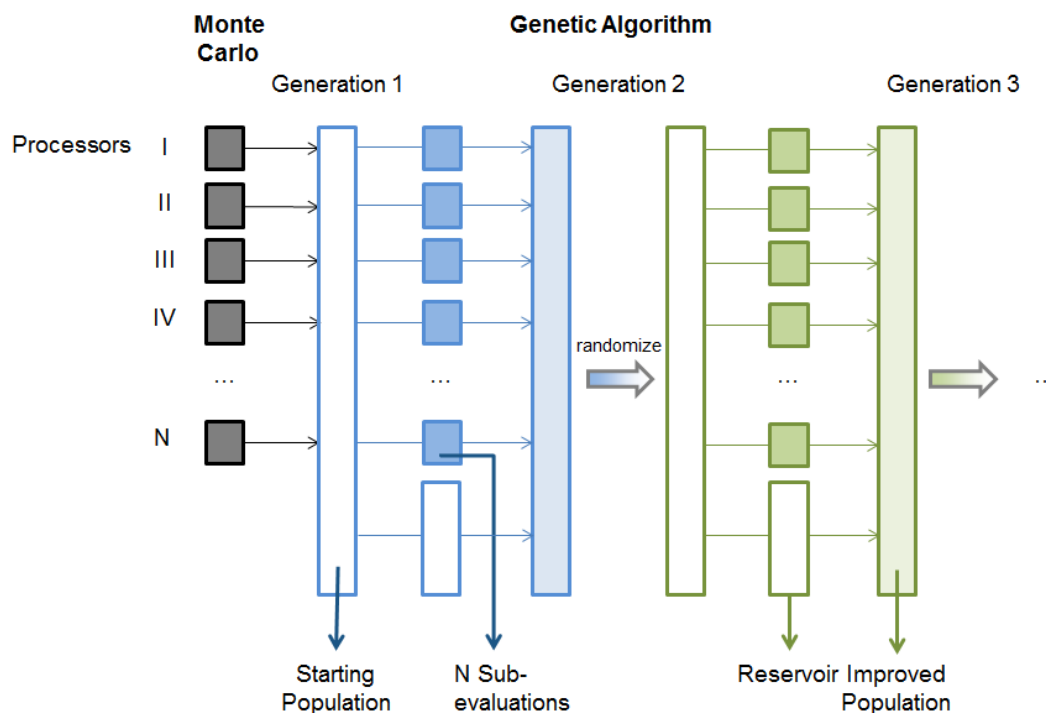


Monte-Carlo Genetic Algorithm



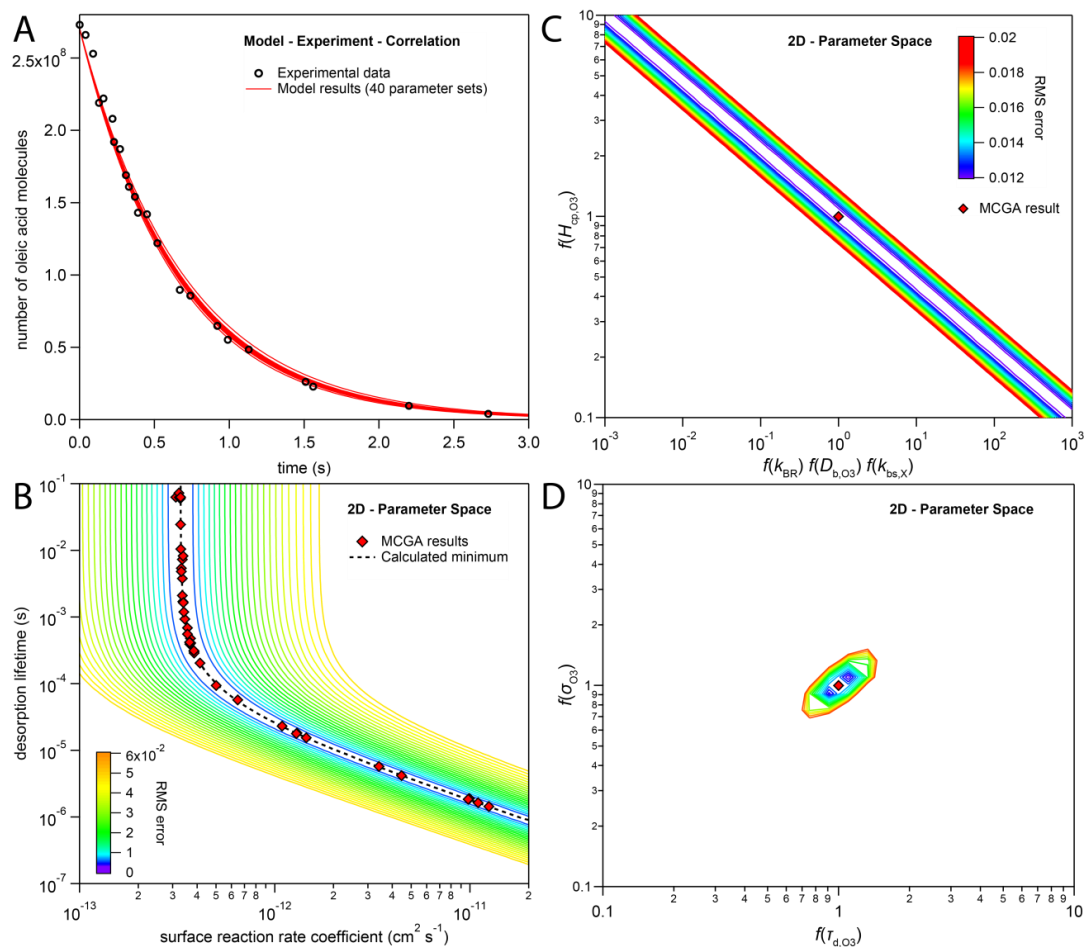
305

306 **Figure 1.** Schematic representation of the MCGA optimization method consisting of a Monte-Carlo
307 sampling, which feeds into a genetic algorithm. Through survival, recombination and mutation steps,
308 ensembles of model input parameter sets are iteratively improved over several generations until a sufficient
309 correlation to the experimental data is obtained.



310

311 **Figure 2.** Schematic visualization of the parallelized MCGA optimization method. The Monte Carlo step
312 is performed independently on N processors and the best fitting parameter sets are fed along with random
313 parameter sets into the starting population. During the genetic algorithm step, each processor extracts a
314 number of parameter sets from the collective pool and performs a sub-evaluation of the genetic algorithm
315 on these parameter sets. After completion, the optimized parameter sets are fed back into the pool, which
316 always contains a non-zero number of parameter sets as reservoir. After randomization, a different
317 combination of parameter sets is extracted and the process repeated.

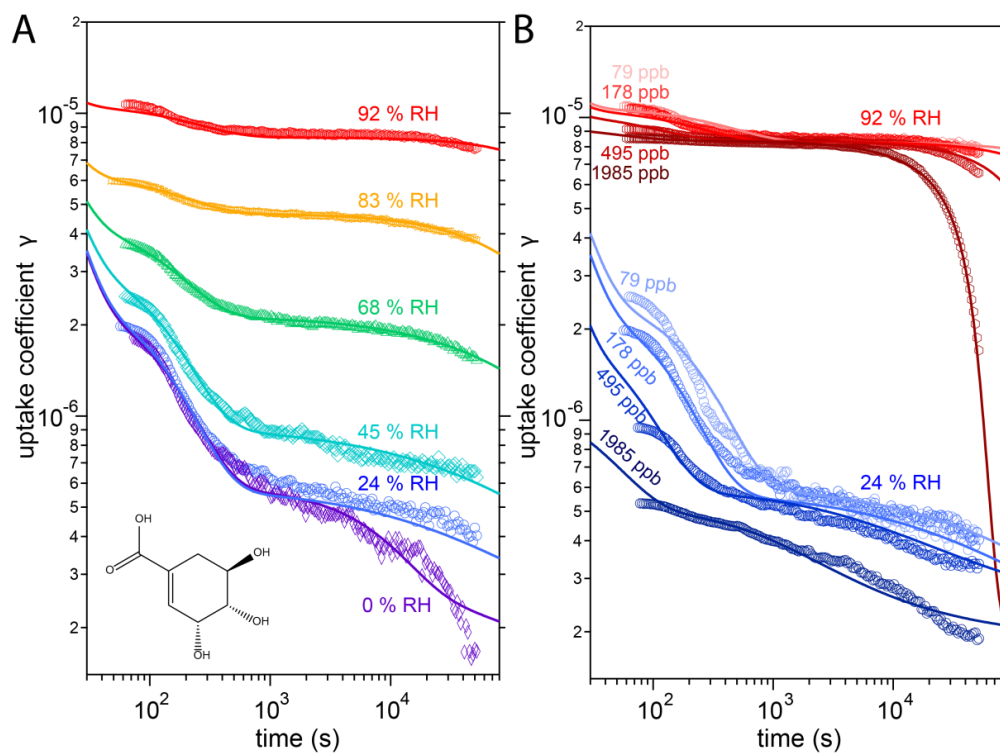


318

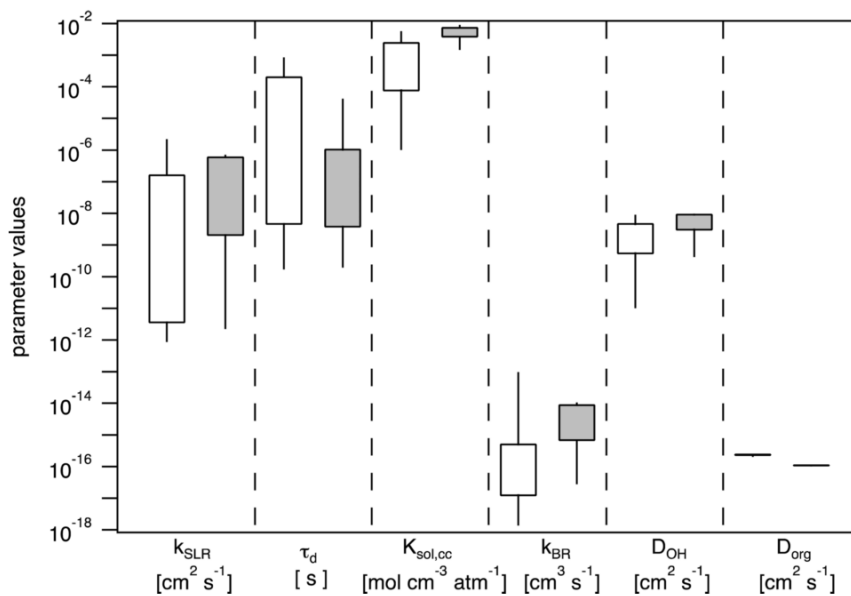
319 **Figure 3.** (A) Results from repeatedly fitting a kinetic model to a single experimental decay curve (adopted
320 from Hearn et al., 2005). MCGA was used to optimize two model parameters, a surface reaction rate
321 coefficient and the desorption lifetime of the gas phase oxidant. All other model parameters remained fixed.
322 (B) Visualization of MCGA algorithm's findings on the 2-dimensional optimization hypersurface. The
323 hypersurface (contour lines represent the root mean square deviances) exhibits no unique minimum due to
324 insufficiently broad experimental data and optimization results (red diamonds) scatter along the extended
325 minimum (black dashed line). (C) and (D) show exemplary optimization hypersurfaces with two parameters



326 showing an elongated (C) or a distinct minimum (D). Panels C and D are reproduced from Berkemeier et
327 al. (2016) with permission from the PCCP Owner Societies.



328
329 **Figure 4.** Observed (markers) and modelled (lines) uptake coefficients of ozone onto a thin film of shikimic
330 acid as a function of exposure time. (A) Uptake coefficients at 178 ppb ozone gas phase concentration $[\text{O}_3]_{\text{g}}$
331 at different relative humidities of 0, 24, 45, 68, 83, and 92%. The structural formula of shikimic acid is
332 displayed in the left bottom corner. (B) Uptake coefficients at 24% RH (blue solid lines) and 92% RH (red
333 solid lines) with different $[\text{O}_3]_{\text{g}}$ of 79, 178, 495, and 1985 ppb. Reproduced from Berkemeier et al. (2016)
334 with permission from the PCCP Owner Societies.



335

336 **Figure 5.** Kinetic parameters for multiphase chemical reactions of OH with levoglucosan (white) and
337 abietic acid (gray) determined by the MCGA method of fitting the experimental data with the KM-GAP
338 model. The ranges of parameters are depicted as a box–whisker plot (the percentiles of 10, 25, 75, and 90%
339 are shown). Reprinted with permission from Arangio et al. (2015). Copyright 2015 American Chemical
340 Society.

341 **References**

- 342 Abbatt, J. P. D., Lee, A. K. Y., and Thornton, J. A.: Quantifying trace gas uptake to tropospheric
343 aerosol: recent advances and remaining challenges, *Chem. Soc. Rev.*, 41, 6555-6581, 2012.
- 344 Ammann, M., and Pöschl, U.: Kinetic model framework for aerosol and cloud surface chemistry
345 and gas-particle interactions - Part 2: Exemplary practical applications and numerical simulations,
346 *Atmos. Chem. Phys.*, 7, 6025-6045, 2007.
- 347 Arangio, A. M., Slade, J. H., Berkemeier, T., Pöschl, U., Knopf, D. A., and Shiraiwa, M.:
348 Multiphase Chemical Kinetics of OH Radical Uptake by Molecular Organic Markers of Biomass
349 Burning Aerosols: Humidity and Temperature Dependence, Surface Reaction, and Bulk Diffusion,
350 *J. Phys. Chem. A*, 119, 4533-4544, 10.1021/jp510489z, 2015.
- 351 Arora, J. S., Elwakeil, O. A., Chahande, A. I., and Hsieh, C. C.: Global optimization methods for
352 engineering applications: A review, *Struct. Optimization*, 9, 137-159, 10.1007/bf01743964, 1995.
- 353 Berkemeier, T., Huisman, A. J., Ammann, M., Shiraiwa, M., Koop, T., and Pöschl, U.: Kinetic
354 regimes and limiting cases of gas uptake and heterogeneous reactions in atmospheric aerosols and
355 clouds: a general classification scheme, *Atmos. Chem. Phys.*, 13, 6663-6686, 10.5194/acp-13-
356 6663-2013, 2013.
- 357 Berkemeier, T., Steimer, S. S., Krieger, U. K., Peter, T., Pöschl, U., Ammann, M., and Shiraiwa,
358 M.: Ozone uptake on glassy, semi-solid and liquid organic matter and the role of reactive oxygen
359 intermediates in atmospheric aerosol chemistry, *Phys. Chem. Chem. Phys.*, 18, 12662-12674,
360 10.1039/C6CP00634E, 2016.
- 361 Cappa, C. D., Zhang, X., Loza, C. L., Craven, J. S., Yee, L. D., and Seinfeld, J. H.: Application of
362 the Statistical Oxidation Model (SOM) to secondary organic aerosol formation from
363 photooxidation of C12 alkanes, *Atmos. Chem. Phys.*, 13, 1591-1606, 10.5194/acp-13-1591-2013,
364 2013.
- 365 Chan, A. W. H., Kroll, J. H., Ng, N. L., and Seinfeld, J. H.: Kinetic modeling of secondary organic
366 aerosol formation: effects of particle- and gas-phase reactions of semivolatile products, *Atmos.*
367 *Chem. Phys.*, 7, 4135-4147, 10.5194/acp-7-4135-2007, 2007.
- 368 Finlayson-Pitts, B. J.: Reactions at surfaces in the atmosphere: integration of experiments and
369 theory as necessary (but not necessarily sufficient) for predicting the physical chemistry of
370 aerosols, *Phys. Chem. Chem. Phys.*, 11, 7760-7779, 10.1039/b906540g, 2009.
- 371 George, I. J., and Abbatt, J. P. D.: Heterogeneous oxidation of atmospheric aerosol particles by
372 gas-phase radicals, *Nat. Chem.*, 2, 713-722, 10.1038/nchem.806, 2010.
- 373 Hanson, D. R., Ravishankara, A. R., and Solomon, S.: Heterogeneous reactions in sulfuric acid
374 aerosols - A framework for model calculations, *J. Geophys. Res. Atmos.*, 99, 3615-3629,
375 10.1029/93jd02932, 1994.
- 376 Hearn, J. D., Lovett, A. J., and Smith, G. D.: Ozonolysis of oleic acid particles: evidence for a
377 surface reaction and secondary reactions involving Criegee intermediates, *Phys. Chem. Chem.*
378 *Phys.*, 7, 501-511, 10.1039/b414472d, 2005.
- 379 Herrmann, H., Ervens, B., Nowacki, P., Wolke, R., and Zellner, R.: A chemical aqueous phase
380 radical mechanism for tropospheric chemistry, *Chemosphere*, 38, 1223-1232, 10.1016/S0045-
381 6535(98)00520-7, 1999.
- 382 Hosny, N. A., Fitzgerald, C., Vysniauskas, A., Athanasiadis, A., Berkemeier, T., Uygur, N.,
383 Pöschl, U., Shiraiwa, M., Kalberer, M., Pope, F. D., and Kuimova, M. K.: Direct imaging of
384 changes in aerosol particle viscosity upon hydration and chemical aging, *Chem. Sci.*,
385 10.1039/C5SSC02959G, 2016.



- 386 Jenkin, M. E., Saunders, S. M., and Pilling, M. J.: The tropospheric degradation of volatile organic
387 compounds: a protocol for mechanism development, *Atmos. Environ.*, 31, 81-104,
388 10.1016/S1352-2310(96)00105-7, 1997.
- 389 Julin, J., Shiraiwa, M., Miles, R. E. H., Reid, J. P., Pöschl, U., and Riipinen, I.: Mass
390 Accommodation of Water: Bridging the Gap Between Molecular Dynamics Simulations and
391 Kinetic Condensation Models, *J. Phys. Chem. A*, 117, 410-420, 10.1021/jp310594e, 2013.
- 392 Kampf, C. J., Liu, F., Reinmuth-Selzle, K., Berkemeier, T., Meusel, H., Shiraiwa, M., and Pöschl,
393 U.: Protein Cross-Linking and Oligomerization through Dityrosine Formation upon Exposure to
394 Ozone, *Environ. Sci. Technol.*, 49, 10859-10866, 10.1021/acs.est.5b02902, 2015.
- 395 Kolb, C. E., Cox, R. A., Abbatt, J. P. D., Ammann, M., Davis, E. J., Donaldson, D. J., Garrett, B.
396 C., George, C., Griffiths, P. T., Hanson, D. R., Kulmala, M., McFiggans, G., Pöschl, U., Riipinen,
397 I., Rossi, M. J., Rudich, Y., Wagner, P. E., Winkler, P. M., Worsnop, D. R., and O' Dowd, C. D.:
398 An overview of current issues in the uptake of atmospheric trace gases by aerosols and clouds,
399 *Atmos. Chem. Phys.*, 10, 10561-10605, 10.5194/acp-10-10561-2010, 2010.
- 400 Lakey, P. S. J., Berkemeier, T., Tong, H., Arangio, A. M., Lucas, K., Pöschl, U., and Shiraiwa,
401 M.: Chemical exposure-response relationship between air pollutants and reactive oxygen species
402 in the human respiratory tract, *Sci. Rep.*, 6, 32916, 10.1038/srep32916, 2016.
- 403 Lowe, S., Partridge, D. G., Topping, D., and Stier, P.: Inverse modelling of Köhler theory – Part
404 1: A response surface analysis of CCN spectra with respect to surface-active organic species,
405 *Atmos. Chem. Phys.*, 16, 10941-10963, 10.5194/acp-16-10941-2016, 2016.
- 406 McNeill, V. F., Woo, J. L., Kim, D. D., Schwier, A. N., Wannell, N. J., Sumner, A. J., and Barakat,
407 J. M.: Aqueous-phase secondary organic aerosol and organosulfate formation in atmospheric
408 aerosols: A modeling study, *Environ. Sci. Technol.*, 46, 8075-8081, 10.1021/es3002986, 2012.
- 409 Partridge, D. G., Vrugt, J. A., Tunved, P., Ekman, A. M. L., Struthers, H., and Sorooshian, A.:
410 Inverse modelling of cloud-aerosol interactions – Part 2: Sensitivity tests on liquid phase clouds
411 using a Markov chain Monte Carlo based simulation approach, *Atmos. Chem. Phys.*, 12, 2823-
412 2847, 10.5194/acp-12-2823-2012, 2012.
- 413 Pöschl, U., Rudich, Y., and Ammann, M.: Kinetic model framework for aerosol and cloud surface
414 chemistry and gas-particle interactions - Part 1: General equations, parameters, and terminology,
415 *Atmos. Chem. Phys.*, 7, 5989-6023, 2007.
- 416 Pöschl, U., and Shiraiwa, M.: Multiphase Chemistry at the Atmosphere–Biosphere Interface
417 Influencing Climate and Public Health in the Anthropocene, *Chem. Rev.*, 115, 4440–4475,
418 10.1021/cr500487s, 2015.
- 419 Riedel, T. P., Lin, Y. H., Zhang, Z., Chu, K., Thornton, J. A., Vizuete, W., Gold, A., and Surratt,
420 J. D.: Constraining condensed-phase formation kinetics of secondary organic aerosol components
421 from isoprene epoxydiols, *Atmos. Chem. Phys.*, 16, 1245-1254, 10.5194/acp-16-1245-2016, 2016.
- 422 Saunders, S. M., Jenkin, M. E., Derwent, R. G., and Pilling, M. J.: Protocol for the development
423 of the Master Chemical Mechanism, MCM v3 (Part A): tropospheric degradation of non-aromatic
424 volatile organic compounds, *Atmos. Chem. Phys.*, 3, 161-180, 10.5194/acp-3-161-2003, 2003.
- 425 Shiraiwa, M., Pfrang, C., and Pöschl, U.: Kinetic multi-layer model of aerosol surface and bulk
426 chemistry (KM-SUB): the influence of interfacial transport and bulk diffusion on the oxidation of
427 oleic acid by ozone, *Atmos. Chem. Phys.*, 10, 3673-3691, 2010.
- 428 Shiraiwa, M., Pfrang, C., Koop, T., and Pöschl, U.: Kinetic multi-layer model of gas-particle
429 interactions in aerosols and clouds (KM-GAP): linking condensation, evaporation and chemical
430 reactions of organics, oxidants and water, *Atmos. Chem. Phys.*, 12, 2777-2794, 10.5194/acp-12-
431 2777-2012, 2012.



- 432 Shiraiwa, M., Yee, L. D., Schilling, K. A., Loza, C. L., Craven, J. S., Zuend, A., Ziemann, P. J.,
433 and Seinfeld, J. H.: Size distribution dynamics reveal particle-phase chemistry in organic aerosol
434 formation, *Proc. Natl. Acad. Sci. USA*, 110, 11746-11750, 10.1073/pnas.1307501110, 2013.
- 435 Shiraiwa, M., Berkemeier, T., Schilling-Fahnestock, K. A., Seinfeld, J. H., and Poschl, U.:
436 Molecular corridors and kinetic regimes in the multiphase chemical evolution of secondary organic
437 aerosol, *Atmos. Chem. Phys.*, 14, 8323-8341, 10.5194/acp-14-8323-2014, 2014.
- 438 Smith, G. D., Woods, E., Baer, T., and Miller, R. E.: Aerosol uptake described by numerical
439 solution of the diffusion - Reaction equations in the particle, *J. Phys. Chem. A*, 107, 9582-9587,
440 10.1021/jp021843a, 2003.
- 441 Steimer, S. S., Berkemeier, T., Gilgen, A., Krieger, U. K., Peter, T., Shiraiwa, M., and Ammann,
442 M.: Shikimic acid ozonolysis kinetics of the transition from liquid aqueous solution to highly
443 viscous glass, *Phys. Chem. Chem. Phys.*, 17, 31101-31109, 10.1039/C5CP04544D, 2015.
- 444 Vieceli, J., Roeselova, M., Potter, N., Dang, L. X., Garrett, B. C., and Tobias, D. J.: Molecular
445 dynamics simulations of atmospheric oxidants at the air-water interface: Solvation and
446 accommodation of OH and O₃, *J. Phys. Chem. B*, 109, 15876-15892, 10.1021/jp051361+, 2005.
- 447 Worsnop, D. R., Morris, J. W., Shi, Q., Davidovits, P., and Kolb, C. E.: A chemical kinetic model
448 for reactive transformations of aerosol particles, *Geophys. Res. Lett.*, 29, 57,
449 10.1029/2002gl015542, 2002.
- 450 Zobrist, B., Soonsin, V., Luo, B. P., Krieger, U. K., Marcolli, C., Peter, T., and Koop, T.: Ultra-
451 slow water diffusion in aqueous sucrose glasses, *Phys. Chem. Chem. Phys.*, 13, 3514-3526,
452 10.1039/c0cp01273d, 2011.
- 453 Zuend, A., and Seinfeld, J. H.: A practical method for the calculation of liquid-liquid equilibria in
454 multicomponent organic-water-electrolyte systems using physicochemical constraints, *Fluid
455 Phase Equilibria*, 337, 201-213, 2013.